Universal Journal of Carbon Research
https://ojs.wiserpub.com/index.php/UJCR/

Research Article

Highly-effective removal of methylene blue dye using Cocoa (*Theobroma cacao L.*) Pods modified with HCl: Optimization using response surface methodology

Kana Dénise Félicité[1], Abdoul Ntieche Rahman[2], Lekene Ngouateu René Blaise[1], Murat Yilmaz[3], Ndi Julius Nsami[1], Kouotou Daouda[1*]

[1]Applied Physical and Analytical Chemistry Laboratory, Department of Inorganic Chemistry, Faculty of Science, P.O. Box 812 Yaoundé, University of Yaoundé I-Cameroon
[2]Department of Chemistry, Higher Teacher Training College Bertoua, The University of Bertoua, PO Box 652, Bertoua, Cameroon
[3]Department of Chemistry and Chemical Processing Technologies, Bahce Vocational School, Osmaniye Korkut Ata University, Osmaniye 80000, Turkey
E-mail: kouotoudaouda@gmail.com

Received: 26 May 2024; **Revised:** 19 July 2024; **Accepted:** 22 July 2024

Abstract: In this study, the cocoa pods modified with hydrochloric acid (CCA) was prepared and used as bio sorbent for methylene blue (MB) removal in aqueous solution. The CCA was characterized by Fourier Transformed Infrared (FT-IR) spectroscopy, Scanning Electron Microscopy (SEM) and pH of point zero charge (pHpzc). The response surface methodology-full factorial design (RSM-FFD) approach was used to investigate the most influential biosorption parameters and optimize their effects on MB adsorbed quantity. The linear and non-linear regression have been used to find the best fit of isotherms and kinetics models. The optimum sorption parameters were found to be 6.0, 240 mg/L and 30 mg for the pH, MB initial concentration and adsorbent dose respectively. Under these optimum conditions, the MB adsorbed quantity was found to be 150.45 mg/g. The RSM-FFD based on the ANOVA revealed that, there was a good fit between the experimental and predicted values respect to the probability ($P<0.05$) and with 95% degree of confidence. The polynomial equation well explained the synergetic and antagonistic effects of examined factors on MB adsorbed quantity onto CCA. The Freundlich, D.K.R and Temkin isotherms models in one hand, the pseudo-first and pseudo-second order kinetics in order hand gave the best fit for the non-linear MB sorption data. These results demonstrated that, the CCA is a promising, low-cost and eco-friend sorbent for dyes remediation in aqueous medium.

***Keywords*:** Bio-adsorbent; Cocoa pods; synthetic dyes; modelling; optimization; pollution

1. Introduction

Nowadays, water pollution became one of the most serious environmental problems that require full attention of scientists and lawmakers. It is well known that surface and groundwater are polluted by inorganic and/or organic substances amongst which dyes pollution occupy a prominent position [1]. Briefly, there are two types of dyes, namely natural and synthetic dyes [2,3,4]. In this study, only the synthetic dyes drawn attention owing to their occurrence use in the textile, leather, paint, food, printing, pharmaceutical and cosmetic industries

Copyright ©2024 Kana Dénise Félicité, et al.
DOI: https://doi.org/10.37256/2220245025
This is an open-access article distributed under a CC BY license
(Creative Commons Attribution 4.0 International License)
https://creativecommons.org/licenses/by/4.0/

[1,5,6,7,8,9]. Among the aforementioned industries, textiles ones are more recognized as the polluting activities of industrial effluent. The synthetic dyes are known to be stable and poorly biodegradable in aqueous medium. There are made of molecules that are readily persistent for a long period time [1,2,5,7,8]. Even at low concentration, synthetic dyes are toxic to aquatic life because they hinder the diffusion of solar light in the water, thus preventing the photosynthesis of aquatic species [10,11] and consequently reducing dissolved oxygen and therefore the overall oxygenation of the water, which endangers the aquatic biotope [1,3,4,12,13,14]. Long-term exposure to synthetic dyes is very damaging for humans and animals and the more visible aspect is the mutagenic and carcinogenic affection [1,2,3,6,7]. This study put an interest on a model dye molecule known with its commercial name as methylene blue and its systematic name, 3,7-bis (dimethylamino) phenothiazin-5-ium chloride [15], which is a basic heterocyclic dye highly soluble in water. It is frequently used in the textile industries to dye silk, cotton, leather, wood, and paper [16]. To limit its presence in effluents and its harmful effects on human health, several techniques and methods have been developed such as coagulation, flocculation, precipitation, membrane filtration, ion exchange, ozonation, irradiation, advanced oxidation processes, electrochemical processes, biodegradation and adsorption [17,18,19]. Most of these techniques and methods are expensive, require a lot of energy, produce secondary products, which require appropriate subsequent treatment [20]. Among the aforementioned treatment processes, adsorption on activated carbon was found to be the most efficient [17]. Additionally, the adsorption technique has the advantage of being less expensive, easy to design and efficient even at low concentrations of pollutants [19, 21]. The use of agricultural residues, available materials, inexpensive and with interesting physicochemical characteristics as bio sorbents of toxic dyes in aqueous solution is increasingly interest and the subject of investigation by researchers [22]. But the several works done in that sense are focused on the use of these agricultural residues as starting materials for the activated carbons preparation and their application for the removal of dyes [4, 23, 24, 25, 26]. Some of our previous works dealing with the methylene blue adsorbents have been done [27, 28], but considering some energetic conditions such as high temperature conditions, chemical consumption can be avoided or limited. In this work, the raw material used as bio-adsorbent is cocoa (*Theobroma cacao L.*) pod husk residue. The cocoa is a cash crop cultivated in seven out of ten regions of Cameroon, which makes Cameroon the fourth largest cocoa producer in the world [29]. The cocoa cultivation generates large amounts of pod waste [30]. Each ton of dry cocoa beans corresponds to approximatively 10 tons of cocoa pod waste [31]. These are unnecessarily dumped or simply burned [32]. So, their use as a bio adsorbent would be an added value to this waste and therefore participates in agricultural residues recovery [33]. Despite the effectiveness of agricultural residues in removing dyes in aqueous media, some modifications of their surface functions have been developed in order to increase their effectiveness [31]. Previous works have been carried out using cocoa pod-based bio adsorbents for the elimination of dyes in water by Pua et al., 2013 [34] who adsorbed methylene blue by cocoa pods treated with sodium hydroxide and Takam et al., 2017 [31] who eliminated Reactive Red II and Azure II by natural and plasma treated cocoa pods. This present work performed the cocoa pods acid treatment in order to increase their adsorption capacity. All the previous biosorption works focused more on obtaining the results rather than controlling the predominant factors that would significantly influence the results found. Consequently, without taking into account the specific effects of each factor and the interactions between factors that act within each other during the adsorption process [35]. In most of the studies found, one factor is set at a certain level by varying the other in order to determine the optimal conditions for adsorption. This way of proceeding has drawbacks such as the absence of information on the interactions between the effects of the factors studied, the high number of experiments to be carried out, which consequently require more time and the use of large quantities of reagents and energy [19, 29, 36]. Thus, it urges to use the response surface methodology (RSM) which is a mathematical and statistical tool that is interested to study any phenomenon that depends on several factors with a view to their modeling [37]. The RSM is useful to minimize the cost and the time; analyze the effects of each variable in order to obtain the optimal condition for response interest with a minimum number of experiments [28]. Hence, the overall objective of this work is to optimize through the response surfaces methodology, the operational condition for the MB elimination in an aqueous solution onto cocoa pods modified with hydrochloric acid.

2. Materials and methods

2.1 *Chemicals*

The methylene blue also called Basic blue 9 (Phenothiazine-5-ium, 3,7-bis(dimethylamino)-, chloride), with molecular formula $C_{16}H_{18}ClN_3S$, color index of 52015, purity of 97% and molecular weight of 316.86 g/mol was purchased from Fluka. The hydrochloric acid (37%) and sodium hydroxide (85.5%) were purchased from Labkem

and AnalaR Normapur compagnies respectively. All the chemicals were of analytical grade and used without purification.

2.2 *Sampling and sorbent preparation*

The cocoa pods were collected in the locality of Makondo, in the Sanaga Maritime division of the Littoral region of Cameroon. The cocoa pods were washed thoroughly with tap water to remove all the dirt then with distilled water, sun-dried and oven-dried (110°C) for 24 hours. When the drying step was achieved, the dried cocoa pods were grinded and sieved to retain only the particle sizes between 75 and 300 µm. This protocol is similar to that described by Njoku et al., 2011, [38]. Subsequently, a similar protocol used by Pua et al., 2013, [34] was followed to modify/treat the cocoa pods surface. In a 250 mL Erlenmeyer flask, 50.0 mL of 0.1 N of hydrochloric acid solution and 5.0 g of cocoa pods were mixed and stirred for 60min followed by extensive washing with distilled water until a neutral pH to remove the excess and unreacted acid. The washed sample was collected and oven-dried at 110°C for 24 hrs. The material obtained was ground in a mortar, labeled as CCA and stored in the desiccator for further applications.

2.3 *Sorbent characterization*

The textural characteristics of the CCA before MB adsorption were obtained using a chemisorption and physisorption surface area analyzer (Micromeritics TriStar 3000). The surface areas of activated carbons were estimated by BET (Brunauer– Emmett–Teller) model with the assumption of the adsorbed nitrogen molecule having a cross sectional area of 0.162 nm^2, while the total pore volume was determined at the relative pressures of 0.01–0.30. The micropore volume and mesopore volume were calculated with standard isotherm: Universal (Harkins, Jura). The surface functional groups of the cocoa pods and acid-treated cocoa pods before and after methylene blue adsorption were assessed using FT-IR spectroscopy on Bruker Alpha-P device with the diffuse reflection acquisition mode and the spectra were recorded using KBr pellets method in absorbance mode over the frequency range of 400-4000 cm^{-1}. The external surface morphology of CCA was visualized by a JEOL scanning electron microscope JSM-5500 operating at 5kV under a gold spray treatment. The pH of point zero charge (pHpzc) of CCA was determined using a drift method. Briefly, a decimolar solution of KNO_3 was prepared and 20mL of solution was taken and placed in seven conical flasks. The pH of each solution in the sealed conical flask was adjusted between 2 and 12 by addition HCl or NaOH solution of 0.1N. Thereafter, the CCA dose of 0.1g was added at each conical flask and left in agitation for 24hrs. When the agitation time was achieved, each final pH was measured and the pHpzc was determinate by plotting the final pH against initial pH. The pHpzc corresponds to the point where the final pH against initial pH crosses the line that is at pH final = pH initial.

2.4 *Methylene blue batch adsorption*

The conventional batch adsorption mode of MB in aqueous solution was carried out by taking various dose of CCA ranging from 0.03 to 0.08g and then introducing them into a closed reactor in the presence of 20.0 mL of MB solution of known concentration varying from 10 to 240 mg/L and at varying pH between 2 to 11. The pH of the solution was adjusted using a Metrhom pH-meter and 0.01 N of HCl and NaOH solutions. The steal reactor and its contents are placed on a multi-station shaker for a fixed period in order to determine the influencing factors at a constant room temperature of 26°C. Subsequently to the agitation, the solutions were filtered and the MB residual concentration was determined using a UV visible spectrophotometer at a maximum wavelength of 660 nm. The MB adsorbed quantity per unit adsorbent dose at equilibrium and at a particular time, t, are calculated by the following Equation (1) and (2) respectively:

$$Q_e = \frac{(C_0 - C_e)}{m} V \quad (1)$$

$$Q_t = \frac{(C_0 - C_t)}{m} V \quad (2)$$

where *Qe* (mg/g) and *Qt* (mg/g) are the MB adsorption quantities at equilibrium and time, t, respectively. *Co*, *Ce* and *Ct* (mg/L) are the initial concentration, equilibrium concentration and concentration at time, of the MB solution respectively. *V* (L) is the volume of the MB solution; *m* (g) is the adsorbent dose. The linear and non-linear equations of isotherms and kinetics models with the respective error functions are compiled in Table 1.

Table 1. Nonlinear and linear equations of isotherm and kinetic models and errors functions

Models	Nonlinear equations	Linear equations
	Isotherms models	
Langmuir	$Q_e = \frac{Q_m K_L C_e}{1 + K_L C_e}$	$\frac{Ce}{Q_e} = \frac{1}{Q_m K_L} + \frac{Ce}{Q_m}$
Freundlich	$Q_e = K_F C_e^{1/n}$	$ln\ Qe = \ln K_F + \left(\frac{1}{n}\right) lnCe$
Tempkin	$Q_e = \frac{RT}{b} \ln (K_T C_e)$	$Q_e = \frac{RT}{b} \ln K_T + \frac{RT}{b} \ln C_e$
DKR	$Q_e = (q_s)\exp(-k_{ad}\left[RTln\left(1 + \frac{1}{C_e}\right)\right]^2)$	$\ln Q_e = \ln Q_m - K_{ad}\left[RTln\left(1 + \frac{1}{C_e}\right)\right]^2$
	Kinetics models	
Pseudo-first order	$Q_t = Q_e[1 - \exp(-k_1 t)]$	$\ln(Qe - Qt) = lnQe - k_1 t$
Pseudo-second order	$Q_t = \frac{Q_e^2 k_2 t}{1 + Q_e k_2 t}$	$\frac{t}{Q_t} = \frac{1}{k_2 Q_e^2} + \frac{t}{Q_e}$
Elovich	$Q_t = \frac{1}{\beta} \ln (1 + \alpha\beta t)$	$Q_t = \frac{1}{\beta} \ln (\alpha\beta) + \frac{1}{\beta} \ln (t)$
Intraparticle diffusion	$Q_t = k_{ip} t^{0.5} + C_0$	//
Errors functions	Correlation coefficient	$R^2 = 1 - \frac{\sum_{i=1}^{n}(Q_{e.exp} - Q_{e.pre})^2}{\sum_{i=1}^{n}(Q_{e.exp} - \overline{Q_{e.exp}})^2}$
	Root-mean-square error	$RMSE = \sqrt{\frac{\sum_{i=1}^{n}(Q_{e.exp} - Q_{e.pre})^2}{n-1}}$
	Chi-square	$\chi^2 = \sum_{i=1}^{n} \frac{(Q_{e.exp} - Q_{e.pre})^2}{Q_{e.exp}}$

α: initial rate parameter, k_{ip}: initial rate constant, K_L: Langmuir constant, β: extent of adsorption parameter, K_F: Freundlich constant, K_T: Tempkin constant, K_{ad}: Dubinin-Radushkevich constant

2.5 *Experimental design*

The optimization and modeling of MB adsorption onto CCA was achieved by the response surface methodology-full factorial design (RSM-FFD) using Minitab16 statistical software (Minitab 16 Inc., USA). The RSM-FFD was used to generate the experimental design matrix based on the three independent parameters gathered in Table 2.

Table 2. Real and coded variables and their levels

Coded variables	Real variables	Levels		
		-1	0	+1
A	pH	2	4	6
B	Initial concentration (mg/L)	100	170	240
C	Adsorbent dose (g)	0.03	0.055	0.08

The objective of using the RSM-FFD was to reduce the total number of experimental runs to achieve the best overall optimization process. The effects of real variables that were: pH, MB initial concentration and adsorbent dose transformed in coded variables that were: (A), (B) and (C) respectively on the investigated response which was the MB adsorbed quantities onto CCA. The main effect of factors, as well as the effect of their interactions on the response, was determined. Two levels with three factors which according to the FFD correspond to eight (08) experiments to which four (04) experiments were added at the center of the experimental design matrix of the MB bioadsorption process. These four experiments helped to access the experimental error and verify the reproducibility of results. Thus, the experimental design matrix with a total of twelve (12) experiments is given in Table 3. In order to predict adsorbed quantity, a mathematical polynomial equation was developed and the regression model was performed by the ANOVA. The resulting mathematical polynomial equation is given by Equation 3:

$$Q_{ads} = X_0 + X_1 A + X_2 B + X_3 C + X_{12} AB + X_{13} AC + X_{23} BC + X_{123} ABC \quad (3)$$

Where, A, B and C, are coded variables of the factors studied; X_0, X_1, X_2 and X_3, are coefficients of the proper factors.; X_{12}, X_{13}, X_{23} and X_{123}, are the interaction coefficients amongst the factors studied.

Table 3. Experimental design matrix for MB adsorption onto CCA with the experimental and predicted values responses

		Variables		Qads (mg/g)	
Run order	pH	Initial concentration (mg/L)	Adsorbent dose (g)	Experimental value	Predicted value
1	2	100	0,03	14.866	14.866
2	6	100	0,03	66.039	66.010
3	2	240	0,03	123.335	123.337
4	6	240	0,03	150.455	150.456
5	2	100	0,08	20.680	20.680
6	6	100	0,08	24.655	24.655
7	2	240	0,08	49.480	49.480
8	6	240	0,08	58.166	58.166
9	4	170	0,055	60.638	60.863
10	4	170	0,055	61.044	60.863
11	4	170	0,055	60.886	60.863
12	4	170	0,055	60.886	60.863

3. Results and Discussion

3.1 *FT-IR, SEM and pHpzc analysis*

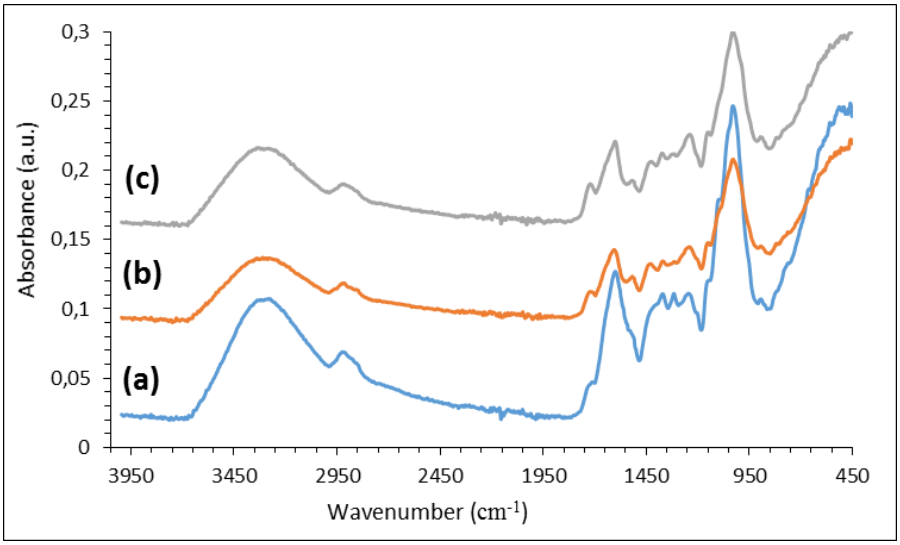


Figure 1. FT-IR spectrum of pristine cocoa pods (a), CCA before MB sorption (b) and CCA after MB sorption (c)

The FT-IR spectra (Figure 1) give the spectrum of virgin cocoa pods (Figure 1a), CCA before the MB adsorption (Figure 1b) and after MB adsorption (Figure 1c). The spectrum of CCA before adsorption (Figure 1b) and that of CCA after adsorption (Figure 1c) show similar absorption bands and the main difference observed is the reduction of the intensities of peaks on CCA compared to that of virgin cocoa pods (Figure 1a). This observation was also made by Martin-Lara et al., 2010 [39] on their work dealing with the treatment of sugar cane bagasse with sulfuric acid, which was concluded to be the cellulose hydrolysis. The broad peak at 3324 cm^{-1} corresponds to the stretching vibration of the O–H bond of water, cellulose and lignin [40]. The band located at 2937 cm^{-1} is attributed to C–H vibration. The observed band at 1732 cm^{-1} is due to C=O stretching vibration. The stretching vibration of N–H coupled with the C–N group is attributed to the peak located at 1620 cm^{-1} [41]. The absorption band at 1261 and 1038 cm^{-1} indicates the presence of C–O and C–N single bonds, respectively. These observations imply the presence of carbonyl groups and therefore the existence on the CCA surface of hydroxyl, carbonyl and carboxyl groups which are well known for their involvement in the adsorption of pollutants [16]. The spectrum of CCA after MB adsorption (Figure 1c) shows conservation of all the adsorption bands of CCA before MB adsorption with an increase in the intensities of some absorption peaks indicating strong interactions between hydroxyl, amine and carboxylic groups located at the surface of the adsorbent and the MB molecules [42]. The SEM images of CCA before MB adsorption (Figure 2a) shows a rough and heterogenous surface, while the surface becomes non-porous but showing grooves after MB adsorption (Figure 2b). The non-porosity of CCA indicates that the adsorption of MB is just related to its surface functional groups. After plotting initial pH against the final ones, as depicted in Figure 4, the pHpzc of CCA was found to be 4.2. Above that value, the surface of the adsorbent material is positively charged and became negative beyond that 4.2. Which means that, the

methylene blue which is a cationic dye, it seems to be adsorbed favorably at pH greater than 4.2 because, there would be electrostatic attraction among negative charge surface and positive species of methylene blue.

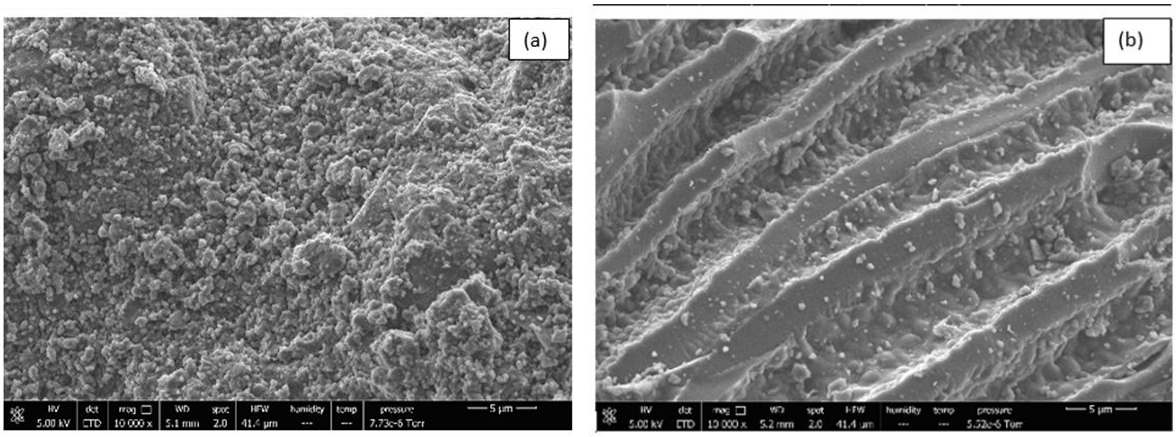


Figure 2. The SEM images of CCA before (a) and after methylene blue adsorption (b)

Table 4. Porous parameters of CCA before adsorption of MB

Sample	BET Surface area (m^2g^{-1})	Micropore volume (cm^3g^{-1})	Cumulative pore volume (cm^3g^{-1})	Cumulative pore area (m^2g^{-1})	Cumulative pore volume (cm^3g^{-1})
CCA	639,78	0,2272	0,2269	60,524	0,067

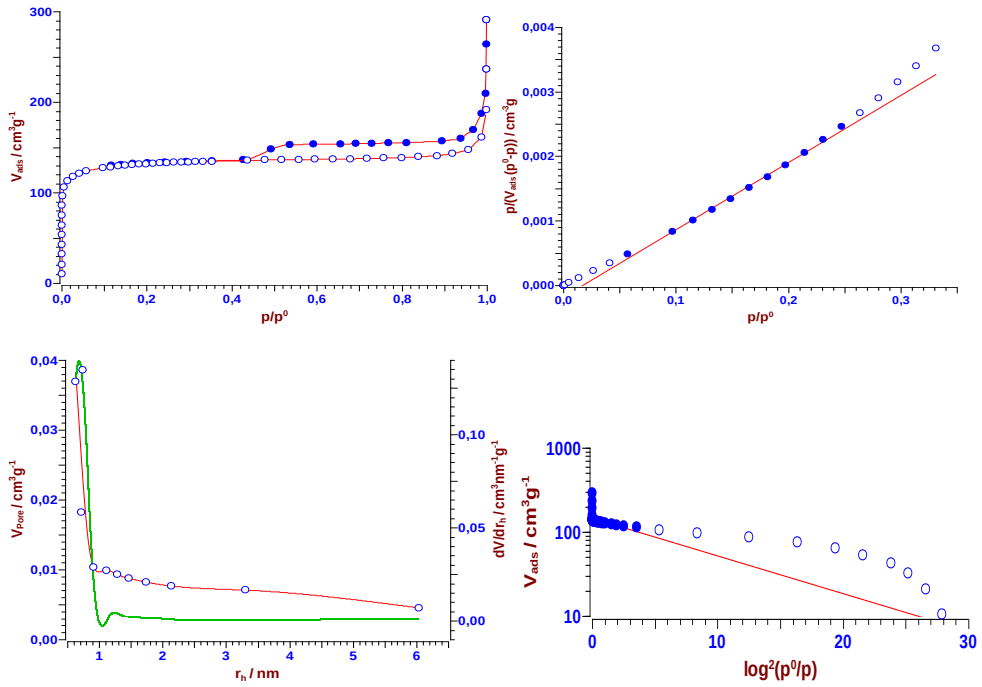


Figure 3. Adsorption–desorption N_2 isotherm of CCA before MB adsorption

Figure 3 shows typical N_2 adsorption–desorption isotherm of the sample of the CCA before MB adsorption. The sample presented greater adsorption capacities at low relative pressures P/Po < 0.1, indicating the presence of a more developed micropore structure; at relative pressure P/Po > 0.1 the filling of external pores by capillary condensation is observed. The isotherm of the CCA sample is of type II with H3 hysteresis according to the IUPAC, which is associated with a narrow pore size distribution of microporous material. The considerable intensity of hysteresis implies the presence of a network of interconnected pores that open onto the surface via external pores. It exhibits the presence of both micropores and mesopores. Table 4 shows that the CCA sample has a specific surface area and micropores volume of 639,78 m^2g^{-1} 78 and 0,2272 cm^3g^{-1} respectively. This shows that the adsorbent prepared has a mixed porous structure.

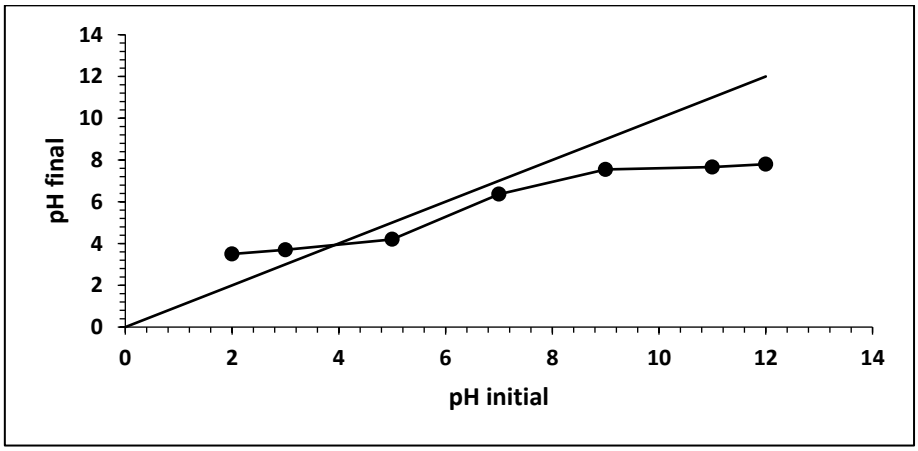


Figure 4. Graph of the pHpzc of CCA

3.2 *Methylene blue batch adsorption analysis*

3.2.1 *Effect of pH*

The effect of pH on MB adsorption onto CCA was done by varying the pH values from 2 to 11 and represented in Figure 5(a). It can be noticed that, the MB adsorbed quantities increase from 11.04 to 11.79 mg/g as well as the increase of pH from 2 to 5. For, pH values greater than 5, the MB adsorbed quantity decreases slightly to 11.74 mg/g showing stabilization. For pH values less than 5 (pH<pHpzc=4.2), the CCA surface is positively charged, therefore, there are electrostatic repulsion with the MB cations. But for pH values greater than 5 (pH>pHpzc=4.2) (figure 4), there are electrostatic attraction between the negative charged surface of CCA and MB cations, thus further increases in the MB sorption [17]. This increase is a consequence of increase in the number of hydroxyl ions on the CCA surface. The stabilization stage observed may be the result of hydroxyl ions saturation onto CCA surface, thus the MB adsorbed amount did not change after. This observation confirms the fact that, the pH is an important adsorption parameter since it affects the surface functional groups of CCA and MB in solution. For the above observation, the optimum pH value was taken to be 6 for the rest of the study.

3.2.2 *Effect of contact time*

Figure 5(b) shows the effect of contact time against the MB adsorbed quantities. It can be observed linear rapid adsorption kinetics which lasts in 5min due the availability of free adsorption sites [20, 43], followed by an equilibrium step after 5 min consequence of reduction of free adsorption sites, causing the retardation of the adsorption process and also to the repulsion between the MB cations on the surface of the material and those in the liquid phase which makes the sites not yet available and difficult to access [44]. The maximum MB adsorbed quantity is 11.78 mg/g which remains almost constant during the time. It takes just 10 min to achieve the equilibrium state and no significant adsorption takes place after 10 min. Hence, the contact time of 10 min was fixed for the kinetic studies as well as the continuation of the experiments.

3.2.3 *Effect of adsorbent dose*

From Figure 5(c), it can be seen that the MB adsorbed amounts decrease with the increase in the adsorbent dose of CCA. This can be due to the fact that the increase in adsorbent dose leads to an increase in electrostatic interactions between the CCA particles which leads to the desorption of MB from the narrow sites of CCA thus causing agglomeration of CCA particles by the formation of aggregates. There is therefore a reduction in the contact surface because the active sites on CCA become hind and an increase in the diffusion path of MB cations into the active sites. This observation is the same trend observed by Abéga et al., 2015 on their work dealing with the C_o (II) and Ni (II) ions adsorption on activated carbon [45].

3.2.4 *Effect of initial concentration*

The effect of initial concentration was studied in the range of 10 to 240 mg/L. It can be seen from Figure 5(d) that, the adsorbed quantity gradually increases until it reaches 94.12 mg/g with the increase in the initial concentration of the solution. This increase could be due to the fact that increasing the MB initial concentration increases also the number of collisions between the MB molecules and CCA particles. This would result in increasing the molecules mobility followed by the collision amongst the molecules themselves [20]. In addition, there are driving forces which are generated to overcome mass transfer resistance between bulk solution and adsorbent surface [21].

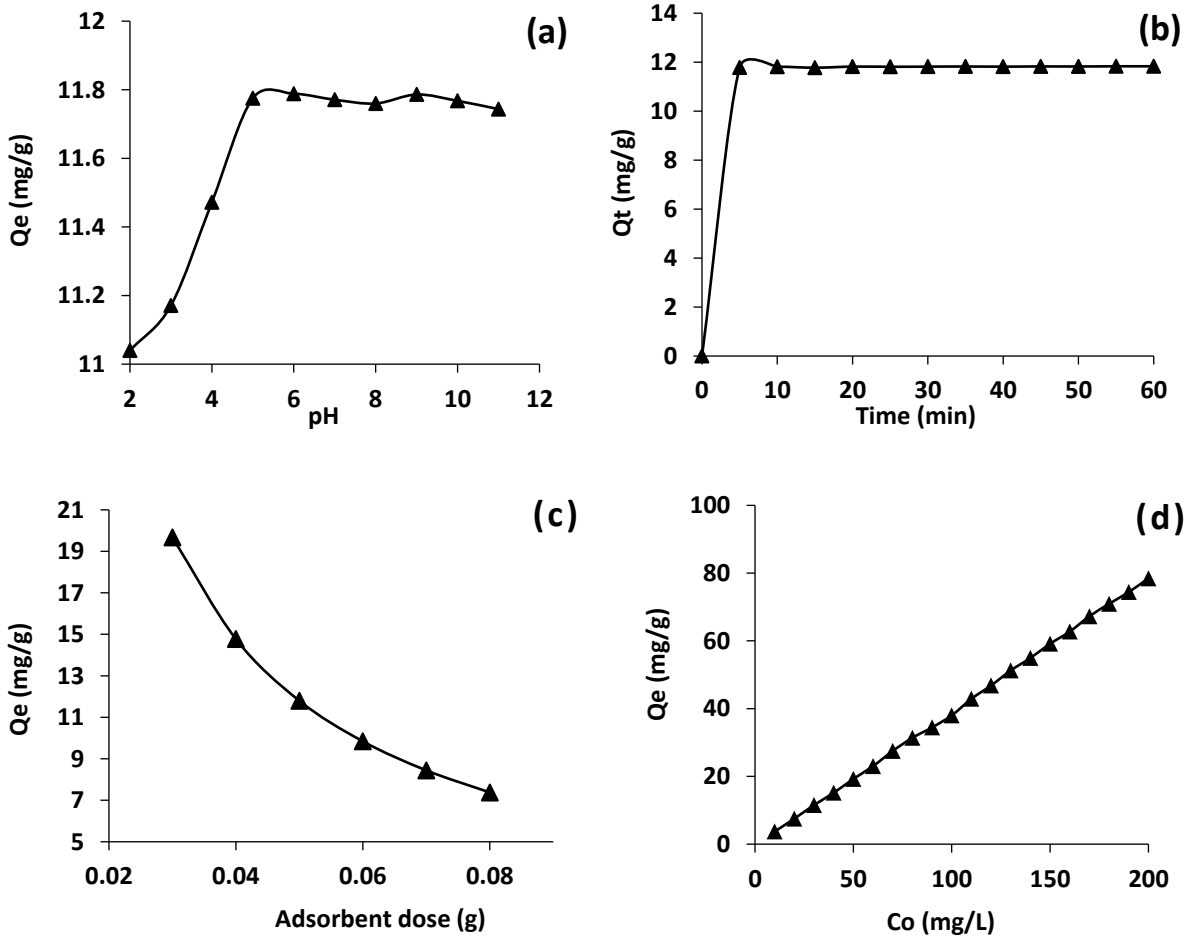


Figure 5. Effects of the pH (m = 0.05 g; C_0 = 30mg/L; t = 20 min) (a); Contact time (m = 0.05 g; C_0 = 30mg/L; pH = 6) (b); Adsorbent dose (pH = 6; C_0 = 30 mg/L; t = 10 min) (c) and initial concentration (m = 0.05 g; pH = 6; t = 10 min) (d)

3.3 *Adsorption isotherms analysis*

The Figure 6 illustrates the fitting of experimental data with linear form of isotherms. Langmuir (Figure 6a); Freundlich (Figure 6b); Tempkin (Figure 6c) and Dubinin-Kaganer-Radushkevich (DKR) (Figure 6d). The linear and nonlinear forms of these isotherm models are gathered in Table 1. The Langmuir isotherm is based on the assumptions that each adsorption site can bind only one entity, the adsorption energy of one entity is the same for all the sites, the adsorption takes place in a monolayer, there is no interaction between the adsorbed molecules [11, 46]. The Freundlich isotherm assumes that adsorption takes place over a heterogeneous surface with uniform adsorption energy and reversible adsorption [47]. The Tempkin isotherm assumes that the adsorption energy of all molecules decreases linearly with layers due to adsorbate-adsorbate interactions, and adsorption is characterized by a uniform distribution of binding energies [48]. The DKR isotherm model gives an idea on the adsorption type that depends on the activation energy [49].

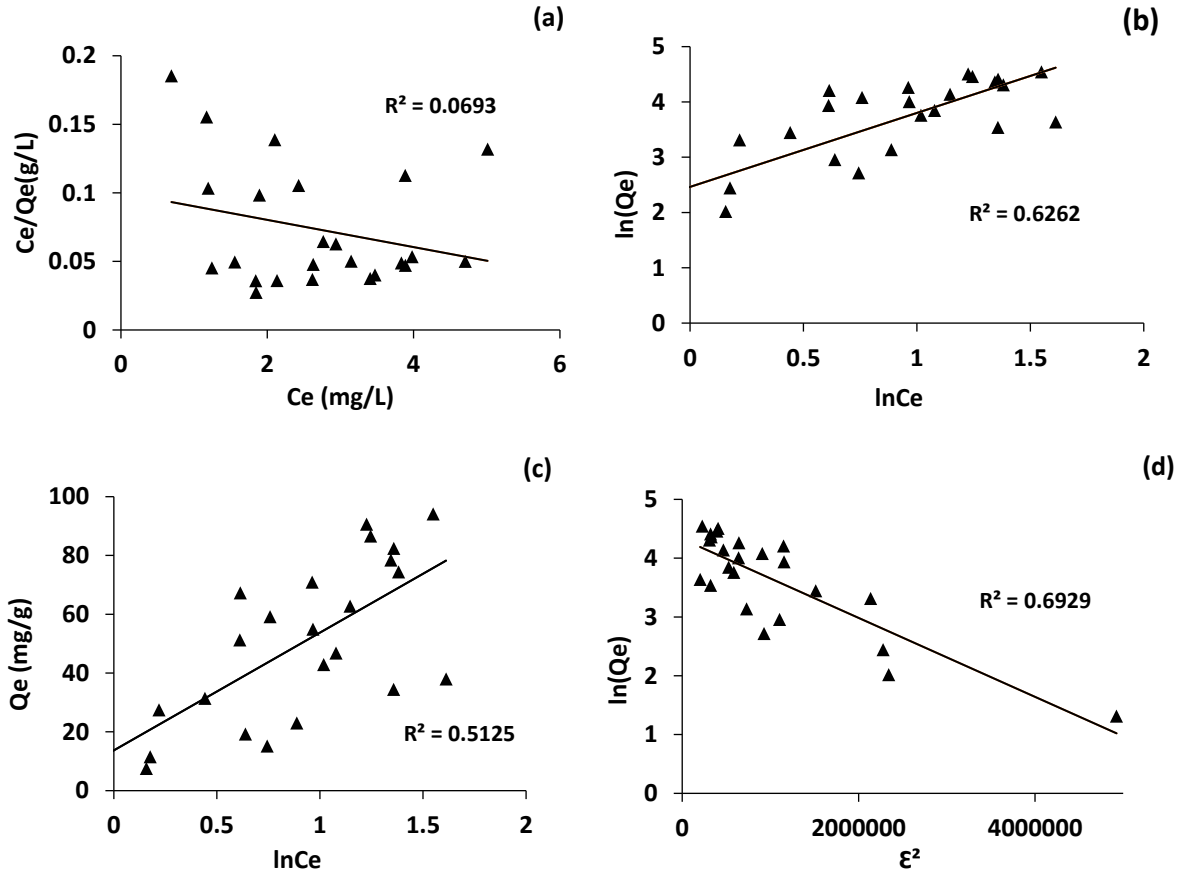


Figure 6. Fitting of Langmuir(a), Freundlich(b), Temkin(c) and D-K-R(d) linear isotherms for MB adsorption onto CCA

The calculated isotherm parameters alongside with their errors function for each isotherm using linear and nonlinear forms equations are tabulated in Table 5. The general observation of Table 5 shows that the linear forms of all the isotherms do not suitably fit the experimental data because of very low values of correlation coefficient R^2 (between 0.0693 and 0.6929), negative values of Langmuir isotherm constant and the high values of *RMSE*. It can be stated that this occurrence resulted could be attributed to an alteration in the error function due to the conversion of a natural nonlinear equation into the linearized form [50]. Thus, it is interesting and important to use the nonlinear forms of different isotherms. All the nonlinear forms of isotherms have R^2 greater than 0.95 excepted Langmuir isotherm (R^2 = 0.4811) indicating that the MB adsorption onto CCA is not taking place on the homogenous surface and that there is the existence of interaction between the MB adsorbed molecules. This assertion is confirmed by the Freundlich isotherm which has the highest R^2 value (0.9963) and the lowest *RMSE* value (1.1553). The limitations of Langmuir and Freundlich isotherms are in their incapability to explain whether the adsorption follows chemical (chemisorption) or physical (physisorption) process. Thus, the calculation of the mean free energy ($E = \frac{1}{(-2\beta)^{1/2}}$) deduced from DKR isotherm model is a useful tool to overcome the aforementioned limitation. According to the mean free energy calculation (E = 722.6803kJ/mol) from MB adsorption onto CCA, it was found that the chemisorption adsorption process was followed since, its mean free energy is greater than 80 kJ/mol [47, 51]. This observation is consistent with the Tempkin constant value (b = 1677.7214J/mol) which possesses a value too high required energy for a process to be called chemisorption.

Table 5. Isotherm parameters for MB adsorption using nonlinear and linear regression

Isotherms models	**Parameters**	**Nonlinear**	**Linear**
	Q_m $(mg.g^{-1})$	216.4258	-101.01
	K_L $(L.mg^{-1})$ $x10^{-3}$	0.1162	-10.12

Langmuir	R^2	0.4811	0.0693
	RMSE	20.5989	160.4171
	χ^2	8141.6213	-5616.4077
	K_F $(L.g^{-1})$	7.5188	11.746
	1/n	1.2225	1.3378
Freundlich	R^2	0.9963	0.6262
	RMSE	1.1553	22.8702
	χ^2	909.4468	253.9979
	q_s $(mg.g^{-1})$	55	75.694
	k_{ad} $(mol^2.J^{-2})$	$9.574x10^{-7}$	7.10^{-7}
D.K.R	E $(kJ.mol^{-1})$	722.6803	0.845
	R^2	0.9853	0.6929
	RMSE	2.2911	31.4027
	χ^2	777.2803	351.4276
	K $(L.mg^{-1})$	6751.9362	1.408
	b $(J.mol^{-1})$	1677.7214	612.2
Tempkin	R^2	0.9724	0.5125
	RMSE	3.1403	41.8228
	χ^2	3090.4093	2377.5783

3.4 *Adsorption kinetics analysis*

In order to determine the MB adsorption mechanism onto CCA, four classical kinetic models (Table 1) were investigated namely, pseudo first-order, pseudo-second-order, Elovich and intraparticle diffusion [15,33]. The values of different kinetic constants for linear and nonlinear kinetics models are compiled in Table 6 and the respective plots are presented in Figure 7. The fitting of data obtained after the study of the effect of contact time on the MB adsorption onto CCA using the linear form showed that only the pseudo-second-order kinetic model was suitable according to its highest value of correlation coefficient closed to unity. The use of nonlinear forms gave better prediction and it can be observed through the MB adsorption which follows the pseudo-first, pseudo-second and Elovich models. It can be seen in Table 5; the above models have $R^2 > 0.99$. The values of *RMSE* and χ^2 for pseudo-first-order are 0.0128 and 0.0002, respectively while those of pseudo-second-order are 0.0121 and 0.0001. These low values of *RMSE* and χ^2 show that the error is evenly distributed and hence, prediction is well balanced [50]. Moreover, the value MB adsorbed quantity (11.786 mg/g) was found to be closed from that calculated from pseudo-first-order (11.813 mg/g) and pseudo-second-order (11.825 mg/g). These observations imply that the number of free sites is significantly greater than the number of MB molecules adsorbed and also indicating that the MB adsorption process onto CCA is following the chemisorption process. The Elovich model confirms the chemical character of the adsorption process on the energetically heterogeneous surface due to its extremely high value of initial adsorption rate coefficient ($\alpha = 6.74x10^{+23}$ $mg.g^{-1}.min^{-1}$) compared to that of desorption rate ($\beta = 5.0424$ $g.min^{-1}$) [41]. The pore diffusion was not the rate-controlling step of the MB adsorption

process according to the low R^2 value (0.8124) of the intra-particular diffusion model. Moreover, the value of constant C_i (5.9763 mg/g) shows that the process was controlled by boundary layer diffusion [50, 51]. The chemisorption process was confirmed on the FT-IR spectrum of CCA after MB adsorption (Figure 1).

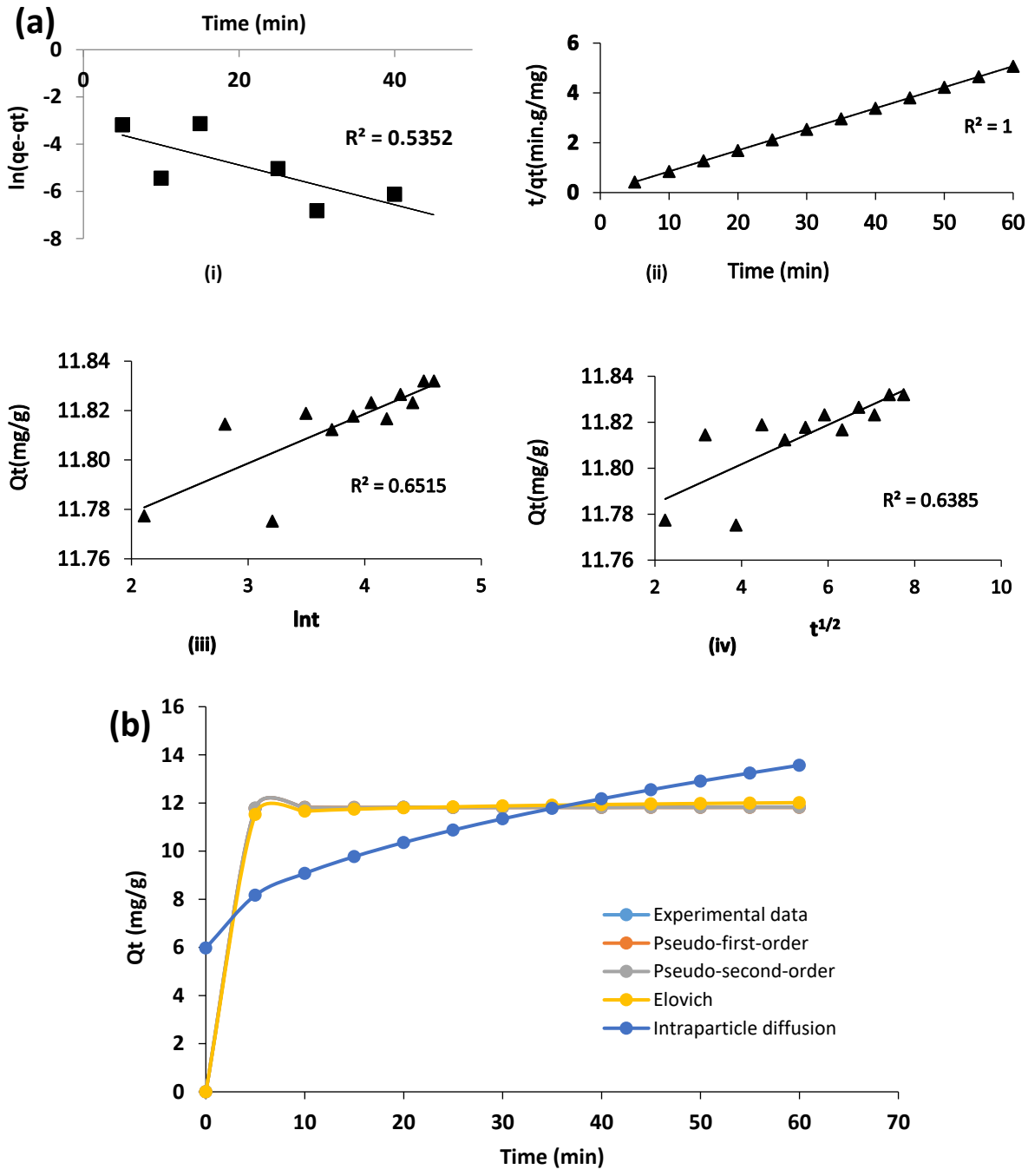


Figure 7. Fitting of linear ((i)-Pseudo first order, (ii)-pseudo second order, (iii)-Elovich, (iv)-Intraparticle diffusion model) (A) and nonlinear forms kinetics models (B) for MB sorption

Table 6. Kinetics parameters for MB adsorption using nonlinear and linear regression

Kinetics models	**Parameters**	**Nonlinear**	**Linear**
Pseudo-first-order	Q_e *(mg/g)*	11.8134	0.0408
	k_1 *(min^{-1})*	1.1572	0.0843

	R^2	0.9999	0.5352
	RMSE	0.0128	30.1627
	χ^2	0.0002	2708.1998
Pseudo-second-order	Q_e *(mg/g)*	11.8248	11.8372
	K_2 *(mg.g^{-1}.min^{-1})*	5.0703	0.5044
	R^2	0.9999	1.0000
	RMSE	0.0121	4.1811
	χ^2	0.0001	11.9833
Elovich	α *(mg.g^{-1}.min^{-1})*	6.7495x10^{+23}	e^{583}
	β *(g.min^{-1})*	5.0424	50.000
	R^2	0.9989	0.6515
	RMSE	0.1101	4.2837
	χ^2	0.0114	12.4448
Intraparticle diffusion	K_{ip} *(mg/g.min$^{1/2}$)*	0.9797	0.0086
	C_i *(mg.g^{-1})*	5.9763	11.767
	R^2	0.8124	0.6385
	RMSE	2.5285	6.2895
	χ^2	3.1932	9.3351

3.5 *Analysis of the optimization of MB adsorption using the RSM-FFD*

3.5.1 *Statistical analysis results and model equation based on the RSM-FFD*

The results obtained after the series of experiments were subjected the ANOVA (analysis of variance) in order to verify the validity of the experimental model chosen using the Minitab 16 software. The ANOVA results are compiled in Table 7.

Table 7. The statistical results analysis of MB adsorption onto CCA

Sources	Degree of freedom	Sum of square	Adjusted sum of square	Adjusted mean square	F-values	P-values
	3	14260.9	14260.9	4753.62	168391.22	0.000
Main effects						
A	1	1033.4	1033.4	1033.40	36607.00	0.000
B	1	8142.6	8142.6	8142.62	288442.23	0.000
C	1	5084.8	5084.8	5084.8	180124.44	0.000
Interaction effets	3	2716.8	2716.8	905.61	32080.24	0.000
A*B	1	46.6	46.6	46.63	1651.68	0.000

A*C	1	538.0	538.0	537.96	19056.53	0.000
B*C	1	2132.3	2132.3	2132.26	75532.52	0.000
Interaction effets	3	103.2	103.21	103.21	3656.23	0.000
A*B*C	1	103.2	103.2	103.21	3656.23	0.000
Residual error	3	0.1	0.1	0.03	//	//
Pure error	3	0.1	0.1	0.03	//	//
R^2 = 100.00%			R^2(adjusted) = 100.00%			

It can be noticed that the high F-values indicate how far the predicted model meet the experimental data satisfactorily. In addition, the probability values P < 0.05 indicate that the model is statistically significant at 95% level of confidence [52]. The ANOVA also provides the residual error value, which measures the variation in data not explained by the model. The model chosen to explain the relationship between the variables studied (pH, MB initial concentration and adsorbent dose) and the response (MB adsorbed quantity) is correct and in agreement with the experimental values obtained. In addition, the high R^2 and adjusted R^2 values obtained show that there is a good correlation between the experimental and predicted values for MB adsorption. According to the results of statistical analysis (Table 7), it emerges that all the linear terms of the factors A (pH), B (MB initial concentration) and C (adsorbent dose), as well as all the terms of the interactions AB (pH-initial concentration), AC (pH-adsorbent dose), BC (initial concentration-adsorbent dose) and ABC (pH-initial concentration-adsorbent dose) are significant because of their respective probability values (P-value <0.05). Thus, the resulting polynomial model from this analysis is represented by Equation (5) giving the adsorbed quantity of MB according to the various parameters in coded variables.

$$Q_{ads} = 63.46 + 11.37A + 31.9B - 25.21C - 2.41AB - 8.2AC - 16.33BC + 3.59ABC \quad (5)$$

Additionally, the observation of the proposed equation shows that, for a confidence level equal to 95%, the coefficients of factors: A (pH), B (initial concentration) and ABC interaction (pH-concentration-mass) are positive. The positive sign in front of a term indicates a synergistic effect, while the negative sign indicates an antagonistic effect on the response investigated [28, 29]. Therefore, these factors (A, B and ABC interaction) have a synergistic effect on MB adsorbed quantity (Qads). This means that they positively influence the MB adsorbed quantity, in other words, their increase, conduct automatically to the increase of MB adsorbed quantity. However, the third factor namely *C* (adsorbent dose) and all the second order interactions AB (pH-concentration), AC (pH-adsorbent mass) and BC (concentration – adsorbent) have a negative sign coefficient. Their influence on the MB adsorbed quantity is therefore negative, thus they have an antagonistic effect on the MB adsorbed quantity. That is, an increase of one of them automatically leads to a decrease in the MB adsorbed amount. The results in Table 7 can also be represented by the Pareto chart diagrams (Figure 8). The Pareto chart represents visually the absolute values of the effects of main factors and the effects of the interaction of factors. A reference vertical line is drawn to indicate that the factors and/or their interaction which extend past this line are potentially significant. Here in this study, the main factors pH (A), initial concentration (B) and mass (C) alongside with their interactions AB, BC, AC and ABC cross the vertical line having thus a significant influence on the response (MB adsorbed quantity, Qads) at the chosen confidence level (α = 0.05). This result confirms the analysis made according to the probability values contain in Table 7.

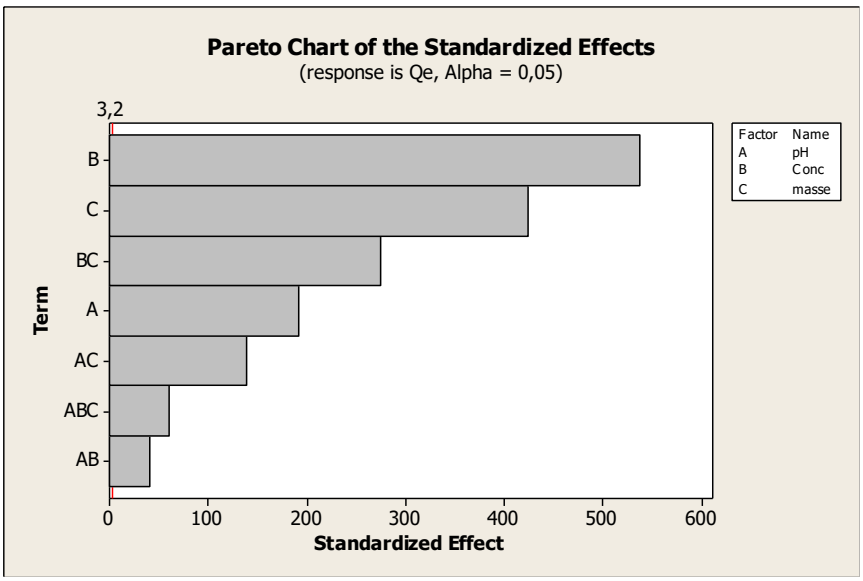


Figure 8. Pareto chart diagram

3.5.2 *Contour plots and response surfaces*

The response surface graphs were plotted using SIGMAPLOT software. Figures 9, 10 and 11 show the relationship of MB adsorbed quantity onto CCA with the pH - initial concentration, pH - adsorbent dose, and initial concentration - adsorbent dose respectively. From Figure 8, the lowest values of Q_e are obtained for low values of pH and initial concentration which means that under these conditions, the number of collisions between molecules is reduced and MB cations compete with hydronium ions, H_3O^+. The large values of Q_e are obtained for high pH and initial concentration values. This could be explained by the increase in the number of hydroxyl ions (OH^-) at the surface of the adsorbent when the pH increases and which creates attractive electrostatic interactions between the negative surface of the bio sorbent and the MB cations in one hand. On the other hand, it is due by the fact that an increase of MB initial concentration increases the number of collisions between the MB molecules on CCA hence Q_e increases. The observation of Figure 10 shows that the MB adsorbed maximum quantity is obtained for small values of CCA adsorbent dose and high pH values. This may be due to the increase in the number of hydroxyl ions on CCA surface when the pH increases which consequently creates attractive electrostatic interactions between the negative CCA surface and MB cations. Moreover, the increase in adsorbent dose leads to a growth of electrostatic interactions between the particles of CCA which leads in turn to MB desorption from the CCA narrow sites thus leading to an agglomeration of the particles of CCA (aggregates formation) and consequently reduces in the contact surface. Figure 11 shows that the maximum MB adsorbed quantity is obtained for small values of CCA dose and at high values of MB initial concentration. Thus, an increase of CCA dose causes agglomeration of CCA particles (aggregates formation) which conducts to a reduction in the contact surface.

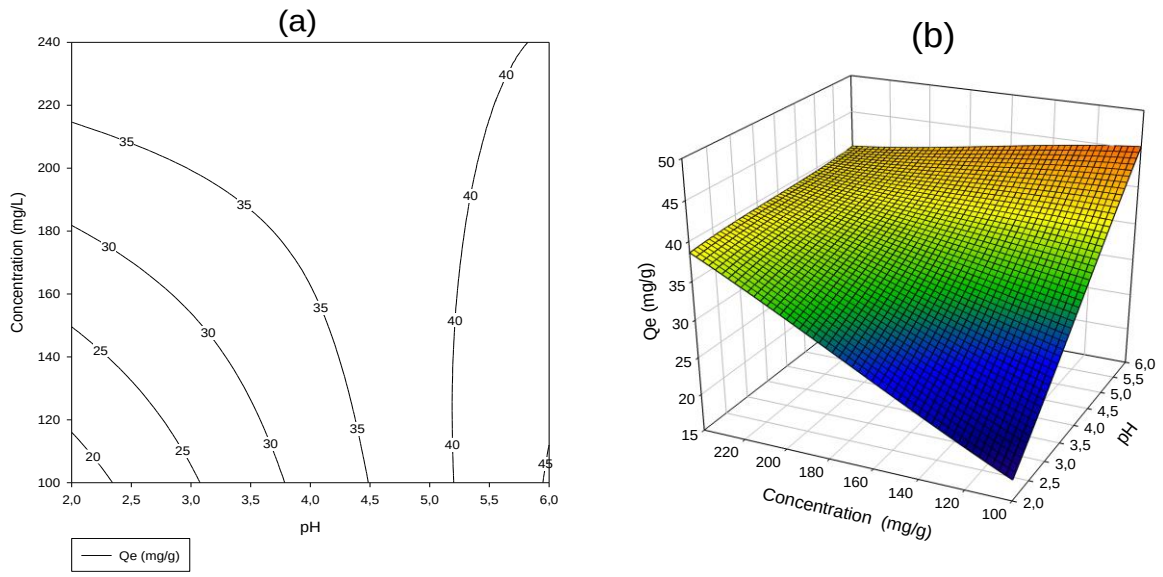


Figure 9. Contour plot (a) and response surface (b) of the interaction initial concentration-pH

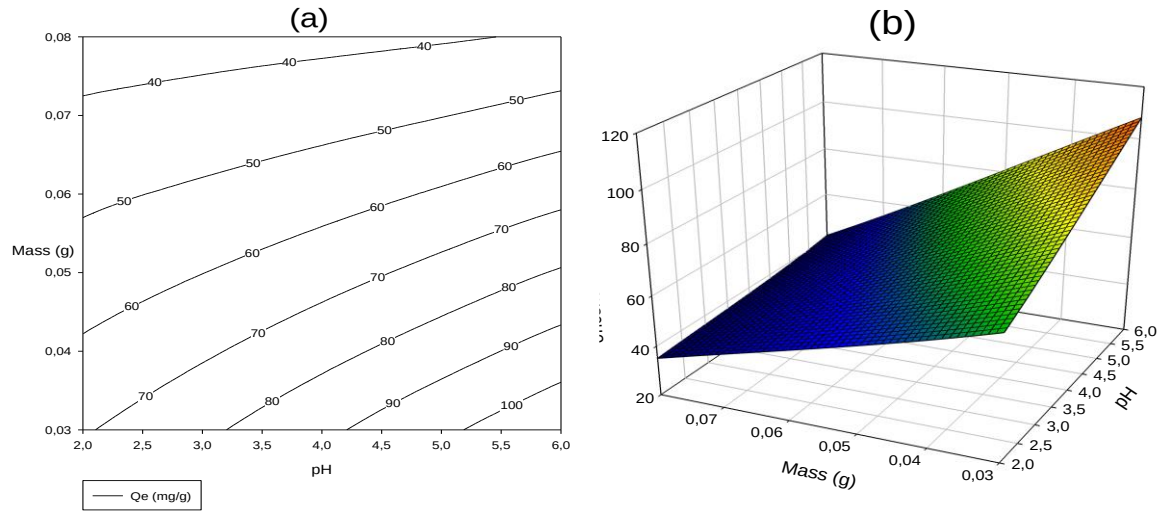


Figure 10. Contour plot (a) and response surface (b) of the interaction adsorbent dose- pH.

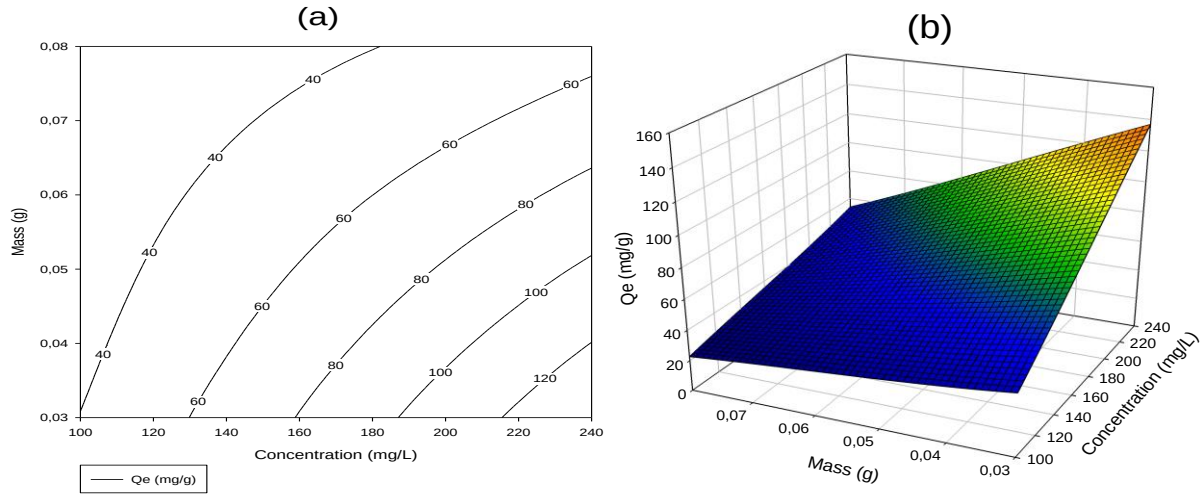


Figure 11. Contour plot (a) and response surface (b) of the interaction adsorbent dose-initial concentration

3.5.3 *Optimum conditions and validation of the model*

The above results showed that the factors that significantly influence the MB adsorption onto CCA are: pH; adsorbent dose and initial concentration. The optimum adsorption conditions searching, that is the values of factors that lead to favorable MB adsorption in the experimental domain is obtained by the superposition of response surface curves (Figures 10(b); 11(b) and 12(b)).

Table 8. Optimum conditions values for MB adsorption onto CCA

Factors	pH	Initial concentration (mg/L)	Adsorbent dose (g)	Predicted response (mg/g)	Experimental response (mg/g)
Levels	+1	+1	-1		
Optimal values	6	240	0.03	150.456	150.455

The obtained condition was recorded in Table 8 and it can be observed that it corresponds to the values 6, 240 mg/L and 0.03 g for the pH, initial concentration and adsorbent dose respectively. These conditions lead to the optimum MB removal value predicted by the polynomial model which found to be 150.456 mg/g and is very closed to the experimental value obtained of 150.455 mg/g. Thus, the experimental value correlates very well with the predicted one with an almost insignificant error (0.066%) thus the model is validated [53]. It can therefore be concluded that the polynomial model used accurately reflects the MB adsorption process involved. The MB removal performance onto the cocoa pods was compared with other adsorbent materials found in literature and

compiled in Table 9. It can be seen from Table 9, that the MB adsorption capacity onto CCA demonstrated a remarkable MB removal ability. This affinity observed by MB with CCA may be the consequence of the acid modification of cocoa pods.

Table 9. Comparison of MB adsorption quantities with other adsorbents

Adsorbents	pH	Temperature (°C)	Adsorbent dose (g)	Initial concentration (mg/L)	Adsorption capacity (mg/g)	Reference
Pig manure biochar	6.5	25	0.3	500	25	[54]
Clay	6	25	0.1	800	210	[55]
Ultrasonic surface modified chitosan	6	25	5 g/L	50 – 200	26.69	[56]
Chitin nanoparticle	6	25	0.015	10	6.90	[57]
Alkaline-treated cocoa pod husk	7	60	0.1	350	263.9	[35]
Sugarcane bagasse	/	25	0.5	50 – 200	17.43	[58]
Citric acid modified kenaf core fibres	7	60	0.1	300	131.6	[59]
Acid modified cocoa pods	6	26	0.03	240	150.45	This work

4. Conclusion

In this study, the cocoa pod was treated using hydrochloric acid to increase its adsorption capacity toward methylene blue in aqueous solution. The investigation of the effects of MB adsorption parameters onto CCA using classical batch adsorption method conducted the maximum MB adsorbed quantity of 11.78 mg/g. The MB adsorption follows the Freundlich, D.K.R and Temkin isotherm models while pseudo-first-order and pseudo-second-order were used to explain the kinetics study. The adsorption of MB on CCA was following was controlled by the chemisorption process. It was observed from isotherm and kinetics studies that the nonlinear forms were giving good predictions compared to the linear forms. The optimization of MB adsorption via the RSM-FFD was a useful tool to understand the interaction effect between the studied factors and to determine the optimal conditions of MB adsorption. The optimal conditions were found to be at pH 6; adsorbent dose of 0.03 g and MB initial concentration of 240 mg/L. From these optimum conditions, the MB adsorbed quantity was found to be 150.455 mg/g which was almost closed to the predicted value (150.456 mg/g). This result showed an insignificant error and the proposed polynomial model correlates very well with the experimental value. Finally, this study revealed that, the cocoa pods modified by hydrochloric acid is an efficient bio sorbent for the removal of organic dyes in liquid effluents. This work is a showcase for future research regarding the use and reuse of bio-adsorbent modified or not against the removal of recalcitrant pollutants from aqueous media.

Acknowledgments

The authors are grateful to the Research Unit: Adsorption and Catalysis of the Applied Physical and Analytical Chemistry Laboratory, Department of Inorganic Chemistry, Faculty of Science of the University of Yaoundé I for providing logistics support.

Conflict of interest

There is no conflict of interest for this study.

References

[1] Olakunle M.O., Inyinbor A.A., Dada A.O. and Bello O.S. Combating dye pollution using cocoa pod husks: a sustainable approach. *International Journal of Engineering*. 2018; **11**: 4-15.
[2] Dastgerdi Z.H., Meshkat S.S., Esrafili M.D. Enhance adsorptive removal of indigo carmine dye performance by functionalized carbon nanotubes based adsorbents from aqueous solution: equilibrium, kinetic, and DFT study. *Journal of Nanostructure in Chemistry*. 2019; **9**: 323–334.
[3] Almoisheer N., Alseroury F. A., Kumar R., Aslamcand M. and Barakat M. A. Adsorption and anion exchange insight of indigo onto CuAl-LDH/SWCNTs nanocomposite: kinetic, thermodynamic and isotherm analysis. *RSC Advances*. 2019; **9**(1): 560-568.
[4] Fatombi J.K., Idohou E.A., Osseni S.A., Agani I., Neumeyer D., Verelst M., Mauricot R. and Aminou T. Adsorption on indigo carmine from aqueous solution by chitosan and chitosan/activated carboncomposite: kinetics, isotherms and thermodynamics studies. *Fibers and Polymers*. 2019; **20**: 1820–1832.
[5] Li Z., Hanafy H., Zhang L., Sellaoui L., Netto M.S., Oliveira M.L.S., Seliem M.K., Dotto G.L., Bonilla-Petriciolet A. and Li Q. Adsorption of congo red and methylene blue dyes on an ashitaba and a walnut shell-based activated carbon from aqueous solutions: Experimental, characterization and advanced modelling. *Chemical Engineering Journal*. 2020. **388**: 124263.
[6] Wang Z., Gao M., Li X., Ning J., Zhou Z. and Li G.Efficient adsorption of methylene blue from aqueous solution by graphene oxide modified persimmon tannins. *Materials Sciences and Engineering*. 2020; **108**: 110196.
[7] Somsesta N., Sricharoenchaikul V. and Aht-Ong D. Adsorption removal of methylene blue onto activated carbon / cellulose biocomposite films: Equilibrium and kinetic studies. *Materials Chemistry and Physics*. 2020; **204**: 122221.
[8] Li Z., Sellaoui L., Dotto G.L., Lamine A.B., Bonilla-Petriciolet A., Hanafy H., Belmabrouk H., Netto M.S. and Erto A. J. interpretation of the adsorption mechanism of reactive black 5 and ponceau 4R dyes on chitosan/polyamide nanofibers via advanced statistical physics model. *Journal of Molecular liquids.* 2019; **285**: 165–170.
[9] Pang X., Sellaoui L., Franco D., Dotto G.L., Georgin J., Bajahzar A., Belmabrouk H., Ben Lamine A., Bonilla-Petriciolet A. and Li Z. Adsorption of crystal violet on biomasses from pecan nutshell, para chestnut husk araucaria bark and palm cactus: experimental study and theoretical modeling via monolayer and double layer statistical physics models. *Chemical Engineering Journal*. 2019; **378**: 122101.
[10] Chatterjee M.J., Ahamed S.T., Mitra M., Kulsi C., Mondal A. and Banerjee D. Visible- light influenced photocatalytic activity of polyaniline-bismuth selenide composites for the degradation of methylene orange, rhodamine B and malachite green dyes. *Applied Surface Science*. 2019; **470**: 472-483.
[11] Wakkel M., Khiari B. and Zagrouba F. Textile wastewater treatment by agro-industrial waste: equilibrium modeling, thermodynamics and mass transfer mechanisms of cationic dyes adsorption onto low cost lignocellulosic adsorbent. *Journal of the Taiwan Institute of Chemical Engineers*. 2019; **96**:439-452.
[12] Chen T., Shi P.H., Zhang J., Li Y., Duan T., Dai L.C., Wang L., Yu X.F., and Zhu W.K. Polymer konjac glucomannan mediated assembly of grapheme oxide as versatile sponges for water pollution control. *Carbohydrate Polymers*. 2018; **202**: 425–433.
[13] Zolgharnein J. and Rastgordani M. Optimization of simultaneous removal of binary mixture of indigo carmine and methyl orange dyes by cobalt hydroxide nano-particles through Taguchi method. *Journal of Molecular Liquid*. 2018; **262:** 405-414.
[14] Gupta T.B. and Lataye D.H. Adsorption of indigo carmine and methylene blue dye: Taguchi's design of experiment to optimize removal efficiency. *Sādhanā*. 2018; **43**(10):170.

[15] Nayak A.K. and Pal A. Green and efficient biosorptive removal of methylene blue by abelmoschus esculentus seed: process optimization and multi-variate modeling. *Journal of Environmental Management*. 2017; **200**: 145-159.
[16] Dallel R., Kesraoui A. and Seffen M. Biosorption of cationic dye onto phragmites australis fibers: characterization and mechanism. *Journal of Environmental Chemical Engineering*. 2018; **6**: 7247-7256.
[17] Kifuani K.M., Mayeko A.K.K., Vesituluta P.N., Lopaka B.I., Bakambo G.E. and Mavinga B.M. Adsorption d'un colorant basique, bleu de methylene, en solution qwueuse, sur un bioadsorbant issu de dechets agricoles de *Cucumeropis mannii Naudin. International Journal of Biological and Chemica Sciences*. 2018; **12**: 558-575.
[18] Meili L., Lins P., Costa M., Almeida R., Abud A. and Soletti Adsorption of methylene blue on agroindustrial wastes: experimental investigation and phenomenological modeling. *Journal of Progress in biophysics and molecular biology*. 2019; **141**: 60-71.
[19] Zhou Y., Lu J., Zhou Y. and Liu Y. Recent advances for dyes removal using novel adsorbant: A revew. *Environnemental Pollution.* 2019; **252**: 352-365.
[20] Ankoro N.O., Kouotou D., Belibi P.D.B., Ndi J.N. and Ketcha J.M. Removal of indigo carmine dye (ic) by batch adsorption method onto dried cola nut shells and its active carbon from aqueous medium. *International Journal of Engineering Sciences and research Technology*. 2016; **5**: 874-87.
[21]. Lekene R.B.N, Kouotou D., Ankoro N.O., Kouoh A.P.-M.S, Ndi J.N. and Ketcha J.M. Development and tailoring of amino-functionalized activated carbon based Cucumerupsi manni Naudin seed shells for the removal of nitrate ions from aqueous solution. *Journal of Saudi Chemical Society*. 2021; **25**: 101316.
[22] Juchen P.T., Piffer H.H., Veit M.T., da Cunha Gonçalves G., Palácio S.M. and Zanette J.C. Biosorption of reactive blue BF-5G dye by malt bagasse: kinetic and equilibrium studies. *Journal of Environmental Chemical Engineering*. 2018; **6**: 7111-7118.
[23] Ankoro N.O., Kouotou D., Lunga P.K., Agbor G.T., Lekene R.B.N., Ndi J.N. and Ketcha J.M. Effet of doping activated carbon based *Ricinodendron Heudelotti* shells with AgNPs on the adsorption of indigo carmine and its anti-bacterial properties. *Arabian Journal of Chemistry*. 2020; **13**: 5241-5253.
[24] Laskar N. and Kumar U. Removal of brilliant green dye from water by modified *Bambusa Tulda*: adsorption isotherm, kinetics and thermodynamics study. *International Journal of Science and Technology*. 2019; **16**: 1649–1662.
[25] Bhomick P.C., Supong A., Baruah M., Pongener C. and Sinha D. Pine cone biomass as an efficient precursor for the synthesis of activated biocarbon for adsorption of anionic dye from aqueous solution: isotherm, kinetic, thermodynamic and regeneration studies. *Sustainable Chemistry and Pharmacy*. 2018; **10**: 41–49.
[26] Danish M. and Ahmad T., Renew. A review on utilization of wood biomass as a sustainable precursor for activated carbon production and application. *Renewable and Sustainable Energy Reviews*. 2018; **87**: 1–21.
[27] Kouotou D., Ngomo H.M., Baçaoui A., Yaacoubi A. and Ketcha J.M. Optimisation of activated carbons prepared by H_3PO_4 and steam activation of oil palm shells. *Journal of Chemistry*. **2013**; article ID 654343: 1-13.
[28] Kouotou D., Ngomo H.M., Baçaoui A., Yaacoubi A. and Ketcha J.M. Physicochemical activation of oil palm shells using response surface methodology: optimization of activated carbons preparation. *International Journal of Current Research*. 2013; **5**: 431-438.
[29] Albadarin A.B., Solomon S., Daher M.A. and Walker G.efficient removal of anionic and cationic dye from aqueous systems using spent Yertba Mate "*llex paraguariensis*" *Journal of the Taiwan Institute of Chimerical Engineers*. 2018; **82**: 144-155.
[30] Mukete N., Li Z., Mukete B. and Bobyeg P. Cocoa production in Cameroon: A socioeconomic and technical efficiency perspective. *International Journal of Agricultural Economics*. 2018; **3**: 1-8.
[31] Yahaya L. and Akinlabi A. equilibrium sorption of lead (II) in aqueous solution onto EDTA-modified cocoa (*Theobroma cocoa*) pod husk residue. *Iranica Journal of Energy* & *Environment*. 2016; **7**: 58-63.
[32] Takam B., Acayanka E., Kamgang G.Y., Pedekwang M.T. and Laminsi S. Enhancement of sorption capacity of cocoa shell biomass modified with non-thermal plasma for removal of both cationic and anionic dyes from aqueous solution. *Environmental Sciences & Pollution Research.* 2017; **24**:16958-16970.
[33] Olu-Owolabi B., Oputu O., Adebowale K., Ogunsolu O. and Olujimi O. biosorption of Cd^{2+} and Pb^{2+} ions into mango stone and cocoa pod waste: kinetic and equilibrium studies. *Scientific research and Essays*. 2012; **7**: 1614-1629.
[34] de Luna M.D.G., Budianta W., Rivera K.K.P. and Arazo R.O. Removal of sodium diclofenac from aqueous solution by adsorbents derived from cocoa pod husks. *Journal of environmental Chemical Engineering*. 2017; **5**: 1465-1474.
[35] Pua F.L., Sajab M.S., Chia C.H., Zakaria S., Rahman I.A. and Salit M.S. Alkalin-treated cocoa pod husk as adsorbent for removing methylene blue from aqueous solutions. *Journal of environmental Chemical Engineering*. 2013; **1**: 460-465.

[36] Lékéné R.B.N., Ndi J.N., Rauf A., Kouotou D., Belibi P.D.B. and Bhanger M.I. Optimization conditions of the preparation of activated carbon based Egusi (*Cucumeropsis mannii Naudin*) seed shells for nitrate ions removal from wastewater. *American Journal of Analytical Chemistry*. 2018; **9**: 439.
[37] Lekene R.B.N., Ankoro N.O., Ndi J.N., Kouotou D., Rahman A.N. and Mbadcam K.J. preparation of activated carbons based balanites aegyptiaca shells by chemical activation: optimization conditions using the methodology of experimental design. *European journal of advanced chemistry research*. 2020; **1**: 1-7.
[38] Morosanu I., Teodosiu C., Coroaba A. and Paduraru C. sequencing batch biosorption of micropollutants from aqueous effluents by rapeseed waste: experimental assessment and statistical modeling. *Journal of Environmental Management*. 2019; **230**: 110-118.
[39] Noormohamadi H.R., Fat'hi M.R., Ghaedi M. and Ghezelbash G.R. Potentiality of White-rot fungi in biosorption of nikel and cadmium: modeling optimization and kinetic study. *Chemosphere*. 2019; **216**: 124-130.
[40] Njoku V., Ayuk A., Ejike E., Oguzie E., Duru C. and Bello O. Cocoa pod husk cost biosorbent for the removal the Pb (II) and Cu (II) from aqueous solution. *Australian Journal of Basic and Applied Sciences*. 2011; **5**: 101-110.
[41] Martín-Lara M.Á., Rico I.L.R., Vicente C.A., García G.B. and de Hoces M.C. Modification of the sorptive characteristics of sugarcane bagasse for removing lead from aqueous solutions. *Desalination*. 2010; **256**: 58-63.
[42] Sayğılı H. and Güzel F. High surface area mesoporous activated carbon from tomato processing solid waste by zinc chloride activation: process optimization, characterization and adsorption. *Journal of Cleaner Production*. 2016; **113**: 995-1004.
[43] Abbas M., Harrache Z., Aksil T. and Trari M. Removal of indigo carmine (IC) in aqueous solution onto activated pomegranate peel (APP) by adsorption process: kinetic and thermodynamic studies. *Journal of Engineered Fibers and Fabrics*. 2021; **17**: 1-10.
[44] Bedin K.C., Martins A.C., Cazetta A.L., Pezoti O. and Almeida V.C. KOH-activated carbon prepared from sucrose spherical carbon: adsorption equilibrium, kinetic and thermodynamic studies for methylene blue removal. *Chemical Engineering Journal*. 2016; **286**: 476-484.
[45] Abéga A.V., Ndi J.N., Ngomo H.M., Kouotou D., Yanou R.N., Ghogomu J.N. and Ketcha J.M. The performance of activated carbon based cola nuts shells for the removal of Co (II) and Ni (II) ion from aqueous solution. *International Journal of Innovative Science, Engineering and Technology*. 2015; **2**: 676-689.
[46] Lekene R.B.N., Sone P.M.A.K., Ndi J.N., Kouotou D., Belibi P.D.B. and Ketcha J.M. Adsorption of phenol and methylene blue onto cola nut shell based activated carbon. *International Journal of Current Research*. 2015; **7**:1-9.
[47] Mehrabi N., Soleimani M., Yeganeh M.M. and Sharififard H. Parameter optimization for nitrate removal from water using activated carbon and composite of activated carbon and Fe_2O_3 nanoparticle. *Royal Society Chemistry Advance*. 2015; **5**: 51470-51482.
[48] Tagne G.M., Ndi J.N. and Ketcha J.M. Adsorption of cooper (II) ions from aqueous solution onto synthetic goethite and two naturally available red soil from Yaoundé- Cameron. *Biotechnology Journal International*. 2013; 221-235.
[49] Rangabhashiyam S., Anu N., Nandagopal M.G. and Selvaraju N. J. Relevance of isotherm models in biosorption of polluants by agricultural by products. *Journal of Environmental Chemical Engineering*. 2014; **2**: 398-414.
[50] Ganguly P., Sarkhel R. and Das P.Synthesis of pyrolyzed biochar and its application for dye removal: batch, kinetic and isotherm with linear and nonlinear mathematical analysis Surfaces *and Interfaces*. 2020; **20**:100616.
[51] Nazir H., Salman M., Athar M., Farooq U., Wahab A. and Akram M. Citric acid functionalized *bougainvillea spectabilis*:a novel, sustainable, and cost-effective biosorbent for removal of heavy metal (Pb^{2+}) from waste water. *Water, Air and Soil Pollution*. 2019; **230**: 1-16.
[52] Asfaram A., Ghaedi M., Dashtian K. and Ghezelbash G.R. preparation and characterization of $Mn_{0.4}Zn_{0.6}Fe_2O_4$ nanoparticles supported on dead cells of *Yarrowia lipolytica* as a novel an efficient adsorbent/biosorbent composite for removal of azo food dyes: central composite design optimization study. *ACS Sustainable Chemistry and Engineering*. 2018; **6**:4549-4563.
[53] Dehghani M.H., Karri R.R., Yeganeh Z.T., Mahvi A.H., Nourmoradi H. and Salari M.Statistical modelling of endocrine disrupting compounds adsorption onto activated carbon prepared from wood using CCD-RSM and DF-hybrid evolutionary optimization framework: comparison of linear and non-linear isotherm and kinetic parameter. *Journal of Molecular Liquids*. 2020; **302**: 112526.
[54] Lonappan L., Rouissi T., Das R.K., Brar S.K., Ramirez A.A., Verma M., Surampalli R.Y. and Valero J.R. Adsorption of methylene blue on biochar microparticles derived from different waste materials. *Waste Manage*. 2016; **49**:537-544.

[55] Fatiha M. and Belkacem B. J.Adsorption of methylene blue from aqueous solution using natural clay. *Journal of Material and environmental Sciences*. 2016; **7**: 285-292.
[56] Dotto G.L., Santos J.M.N., Rodrigues I.L., Rosa R., Pavan F.A. and Lima E.C. Adsorption of methylene blue by ultrasonic surface modified chitin. *Journal of colloid and interface Science.* 2015; **446**: 133-140.
[57] Dhananasekaran S., Palanivel R. and Pappu S. J. Adsorption of methylene blue, bromophenol blue and coomassie brilliant blue by α-chitin nanoparticles. *Journal of Advance Research*. 2016; **7**: 113-124.
[58] Meili L., Lins P.V.S., Costa M.T., Almeida R.L., Abud A.K.S., Soletti J.I., Dotto G.L., Tanabe E.H., Sellaoui L., Carvalho S.H.V. and Erto A. Adsorption of methylene blue on agroindustrial wastes: experimental investigation and phenomenological modeling. *Progress in Biophysics and Molecular Biology*. 2019; **141**, 60-71.
[59] Sajab M.S., Chia C.H., Zakaria S., Jani S.M., Ayob M.K., Chee K.L., Khiew P.S. and Chiu W.S. Citric acid modified kenaf core fibres for removal of methylene blue from aqueous solution. *Bioresource Technology*. 2011; **102**: 7237-7243.